

Journal of Visualized Experiments

A Fibrin-Enriched and tPA-Sensitive Photothrombotic Stroke Model

--Manuscript Draft--

Article Type:	Methods Article - JoVE Produced Video
Manuscript Number:	JoVE61740R2
Full Title:	A Fibrin-Enriched and tPA-Sensitive Photothrombotic Stroke Model
Corresponding Author:	Chia-Yi (Alex) Kuan, MD, PhD University of Virginia School of Medicine Charlottesville, VA UNITED STATES
Corresponding Author's Institution:	University of Virginia School of Medicine
Corresponding Author E-Mail:	alex.kuan@virginia.edu
Order of Authors:	Yi-Min Kuo Yu-Yo Sun Chia-Yi (Alex) Kuan, MD, PhD
Additional Information:	
Question	Response
Please indicate whether this article will be Standard Access or Open Access.	Standard Access (US\$2,400)
Please indicate the city, state/province, and country where this article will be filmed . Please do not use abbreviations.	Charlottesville, Virginia 22902 USA
Please confirm that you have read and agree to the terms and conditions of the author license agreement that applies below:	I agree to the Author License Agreement
Please specify the section of the submitted manuscript.	Medicine
Please provide any comments to the journal here.	

TITLE:

A Fibrin-Enriched and tPA-Sensitive Photothrombotic Stroke Model

AUTHORS AND AFFILIATIONS:

Yi-Min Kuo¹, Yu-Yo Sun², Chia-Yi Kuan²

¹Department of Anesthesiology, Taipei Veterans General Hospital, National Yang-Ming University School of Medicine, Taipei, Taiwan

²Department of Neuroscience, Center for Brain Immunology and Glia (BIG), University of Virginia School of Medicine, Charlottesville, VA

Corresponding Author:

Chia-Yi Kuan (alex.kuan@virginia.edu)

Email Addresses of Co-authors:

Yi-Min Kuo (ymkuo@vghtpe.gov.tw)

Yu-Yo Sun (yuyosun42@virginia.edu)

KEYWORDS:

rose bengal, thrombin, tPA, fibrin, platelets, thrombolysis

SUMMARY:

Traditional photothrombotic stroke (PTS) models mainly induce dense platelet aggregates of a high resistance to tissue plasminogen activator (tPA)-lytic treatment. Here a modified murine PTS model is introduced by co-injecting thrombin and photosensitive dye for photoactivation. The thrombin-enhanced PTS model produces mixed platelet:fibrin clots and is highly sensitive to tPA-thrombolysis.

ABSTRACT:

An ideal thromboembolic stroke model requires certain properties, including relatively simple surgical procedures with low mortality, a consistent infarction size and location, precipitation of platelet:fibrin intermixed blood clots similar to those in patients, and an adequate sensitivity to fibrinolytic treatment. The rose bengal (RB) dye-based photothrombotic stroke model meets the first two requirements but is highly refractory to tPA-mediated lytic treatment, presumably due to its platelet-rich, but fibrin-poor clot composition. We reason that combination of RB dye (50 mg/kg) and a sub-thrombotic dose of thrombin (80 U/kg) for photoactivation aimed at the proximal branch of middle cerebral artery (MCA) may produce fibrin-enriched and tPA-sensitive clots. Indeed, the thrombin and RB (T+RB)-combined photothrombosis model triggered mixed platelet:fibrin blood clots, as shown by immunostaining and immunoblots, and maintained consistent infarct sizes and locations plus low mortality. Moreover, intravenous injection of tPA (Alteplase, 10 mg/kg) within 2 h post-photoactivation significantly decreased the infarct size in T+RB photothrombosis. Thus, the thrombin-enhanced photothrombotic stroke model may be a useful experimental model to test novel thrombolytic therapies.

INTRODUCTION:

Endovascular thrombectomy and tPA-mediated thrombolysis are the only two U.S. Food and Drug Administration (FDA)-approved therapies of acute ischemic stroke, which afflicts ~700,000 patients annually in the United States¹. Because the application of thrombectomy is limited to large vessel occlusion (LVO), while tPA-thrombolysis may alleviate small vessel occlusions, both are valuable therapies of acute ischemic stroke². Moreover, the combination of both therapies (e.g., initiation of tPA-thrombolysis within 4.5 hours of stroke onset, followed by thrombectomy) improves reperfusion and the functional outcomes³. Thus, optimizing thrombolysis remains an important goal for stroke research, even in the era of thrombectomy.

Thromboembolic models are an essential tool for preclinical stroke research aiming to improve thrombolytic therapies. This is because mechanical vascular occlusion models (e.g., intraluminal suture MCA occlusion) do not produce blood clots, and its fast recovery of cerebral blood flow after the removal of mechanical occlusion is overly idealized^{4,5}. To date, major thromboembolic models include photothrombosis⁶⁻⁸, topical ferric chloride (FeCl₃) application⁹, microinjection of thrombin into the MCA branch^{10,11}, injection of ex vivo (micro)emboli into the MCA or common carotid artery (CCA)¹²⁻¹⁴, and transient hypoxia-ischemia (tHI)¹⁵⁻¹⁸. These stroke models differ in the histological composition of ensuing clots and the sensitivity to tPA-mediated lytic therapies (**Table 1**). They also vary in the surgical requirement of craniotomy (needed for in situ thrombin injection and topical application of FeCl₃), the consistency of infarct size and location (e.g., CCA-infusion of microemboli yield very variable outcomes), and global effects on the cardiovascular system (e.g., tHI increases the heart rate and cardiac output to compensate for hypoxia-induced peripheral vasodilation).

The RB dye-based photothrombotic stroke (PTS) model has many attractive features, including simple craniotomy-free surgical procedures, low mortality (typically < 5%), and a predictable size and location of infarct (in the MCA-supplying territory), but it has two major limitations.⁸ The first caveat is weak-to-nil response to tPA-mediated thrombolytic treatment, which is also a drawback of the FeCl₃ model^{7,19,20}. The second caveat of PTS and FeCl₃ stroke models is that the ensuing thrombi consist of densely-packed platelet aggregates with a small amount of fibrin, which not only lead to its resilience to tPA-lytic therapy, but also deviates from the pattern of intermixed platelet:fibrin thrombi in acute ischemic stroke patients^{21,22}. In contrast, the in situ thrombin-microinjection model mainly comprises polymerized fibrin and a uncertain content of platelets¹⁰.

Given the above reasoning, we hypothesized that admixture of RB and a sub-thrombotic dose of thrombin for MCA-targeted photoactivation through thinned skull may increase the fibrin component in the resultant thrombi and boost the sensitivity to tPA-mediated lytic treatment. We have confirmed this hypothesis,²³ and herein we describe detail procedures of the modified (T+RB) photothrombotic stroke model.

PROTOCOL:

This protocol is approved by the Institutional Animal Care and Use Committee (IACUC) at the

University of Virginia and follows the National Institutes of Health Guideline for Care and Use of Laboratory Animals. **Figure 1A** outlines the sequence of surgical procedures of this protocol.

1. Surgery setup

1.1. Place a warming pad with temperature setting at 37 °C on the small animal adaptor at least 15 minutes before the surgery. Prepare a nose-clip roll for adaptor which allows the animal head rotation. Prepare the anesthetics Ketamine (60 mg/kg)/ Xylazine (10 mg/kg).

1.2. Sterilize the surgical tools including scissors, forceps, micro-needle holders, hemostats, cotton swabs and sutures with autoclave (121 °C at 15 psi for 60 min). Prepare tissue glue and eye ointment. Prepare the 532 nm laser protection goggle for surgeons.

1.3. Set up the illumination system with a 532 nm laser source. Prepare a dental drill.

1.4. Prepare the Rose Bengal solution in saline (10 mg/mL). Place an aliquot bovine thrombin (0.1 U/ μ L) on ice-bucket.

1.5. Inject Meloxicam (4.0 mg/kg) subcutaneously to the mouse as analgesia at 30 min before surgery.

2. Ligation of the ipsilateral common carotid artery

2.1. Anesthetize 10-14 week-old male C57BL/6 mice weighing 22 to 30 g by intramuscular injection of Ketamine (60 mg/kg) and Xylazine (10 mg/kg).

2.2. Squeeze the mouse hindlimb to ensure the animal is fully sedated. Remove the hair on left neck and head with the hair removal cream.

2.3. Place the mouse on the small animal adaptor in the supine position. Sterilize the surgical area by wiping skin with three alternating swipes of povidone-iodine and 70% ethanol.

2.4. Under dissecting microscope, make a 0.5 cm left-cervical incision using a pair of micro-scissors and straight forceps at about 0.2 cm lateral to the midline.

2.5. Use a pair of fine serrated forceps to pull apart the soft tissue and fascia to expose the left common carotid artery (LCCA). Carefully separate the left CCA from the vagal nerve using a pair of fine smooth forceps.

2.6. Place a permanent double-knot suture around the LCCA using 5-0 silk suture cut into 20 mm segments, and then close the wound using tissue glue.

3. Skull thinning above the MCA branch and photoactivation

3.1. Flip the mouse to prone position on the small animal adaptor. Rotate the nose-clip roll for 15°. Sterilize the surgical area by wiping skin with three alternating swipes of betadine and 70% ethanol.

3.2. Make a 0.8 cm incision in the scalp using a pair of micro-scissors and straight forceps along the left eye and ear to expose the temporalis muscle, which is located between the eye and the ear (Figure 1B).

3.3. Under the dissecting microscope, make a 0.5 cm incision along the edge of temporalis muscle on left parietal bone by a pair of fine serrated forceps. Make a second 0.3 cm vertical incision on temporalis muscle by a micro scissors. Retract the temporal muscle to expose the edge of parietal bone and squamosal bone. Make sure to visualize the landmark of coronal suture between the frontal and the parietal bones (Figure 1B,C).

3.4. Moisture the skull by applying sterile saline to reveal the left MCA. Mark the proximal MCA branch on the squamosal bone with a marker pen. Gently draw a circle for about 1 mm in diameter surrounding the marked area with the pneumatic dental drill (burr speed setting at 50% of speed controller), and then thin the skull about 0.2 mm in depth without touching the underneath dura. Stop the drilling until a very thin layer of bone is left.

3.5. Mix the thrombin (T, 0.1 U/ μ L, 80 U/kg) and Rose bengal (RB, 10 mg/mL, 50 mg/kg) solution based on the mouse's body weight. For example, for a mouse of 25 g body weight, mix 20 μ L of thrombin (0.1 U/ μ L) and 125 μ L of RB (10 mg/mL).

3.6. Slowly inject T+RB solution (145 μ L per 25 g body weight) into the retro-orbital sinus with an insulin syringe (#31G needle).

NOTE: In pilot experiments, the mortality rate of increasing doses of thrombin mixed with the standard dose of RB dye (50 mg/kg) was examined for photoactivation. The mortality was 0% for 80 U/kg thrombin (n=13), 43% for 120 U/kg thrombin (n=7), and 100% for both 160 U/kg (n=5) and 200 U/kg thrombin (n=5). A dose of 80 U/kg thrombin was therefore chosen for this model. Laser speckle contract imaging was also used to exclude the possibility of rampant blood clotting near the orbital cavity after retro-orbital sinus injection of T+RB (Supplementary Figure 1), as well as, widespread fibrin deposition in the contralateral hemisphere that was not subjected to laser illumination (Supplementary Figure 2).

3.7. Apply eye ointment on both eyes to prevent dryness.

3.8. Apply the illuminator with a 532 nm laser light (with 0.5 mW energy) on the drilled site with 2-inch distance for 20 min. Visualize the illumination on the proximal branch of MCA through a laser protection goggle (Figure 1C, D).

NOTE: The MCA with 532 nm illumination shows red fluorescence under the goggle. The distal MCA will disappear after 10 min illumination. Exclude the animal if the distal MCA flow is still present after 20 min illumination.

3.9. Stop the laser illumination after 20 min. Close the wound with tissue glue and place the animal back to a warm cage for recovery.

3.10. Monitor the mice for 5-10 min until they recover from anesthesia. Place wetted food in the cage and return it to the animal care facility.

4. Intravital imaging (optional)

NOTE: To characterize the thrombus formation in-vivo, use intravital imaging by a spin-disk confocal with photoactivation system²³.

4.1. Make a cranial window ~3 mm in diameter on the parietal bone of skull.

4.2. Place a coverglass on the cranial window and locate the distal MCA (~50 μ m in diameter) under a 20x water-immersion objective.

4.3. Label the circulating platelet by tail vein injection of DyLight488-conjugated anti-GPIIb/IIIa antibody (0.1 mg/kg) at 5 min before imaging.

4.4. Inject the mixture solution of thrombin (80 U/kg) and Rose bengal (50 mg/kg) by retro-orbital at 5 min before imaging.

4.5. Photoactivate the MCA using a 561 nm laser system with laser beam 10 μ m in diameter and record the image until the thrombus formation.

5. tPA administration

5.1. Place the anesthetized animal on a 37 °C warm pad. At the selected post-photoactivation time-point, wet a gauze with ~45 °C warm water and wrap it on the tail for 1 min.

5.2. Inject recombinant human tPA (10 mg/kg) through the tail vein with a 50% bolus and 50% over 30 min by infusion pump.

NOTE: Although the clinical dose of recombinant human tPA for acute ischemic stroke treatment is 0.9 mg/kg, a higher dose (10 mg/kg) is commonly used in rodents to compensate for reduced cross-species tPA reactivity. We also followed the standard protocol of tPA-administration in preclinical stroke models, using 50% as a bolus and 50% infused through the tail vein over 30 min.²⁴

6. Monitor of cerebral blood flow (CBF)

NOTE: To confirm CBF recovery after tPA treatment, use a two-dimensional laser speckle contrast imaging system¹⁵ and record immediately after photothrombosis (step 3.9) or at 24 h after tPA treatment.

6.1. Place anesthetized animal in the prone position and make a midline incision on the scalp with the skull exposed.

6.2. Moisturize the skull with sterile saline and gently apply the ultrasound gel on the skull. Avoid any hair and bubble in the gel, which will interfere the CBF signal.

6.3. Monitor CBF in both cerebral hemispheres under laser speckle contrast imager for 10 min.

6.4. After recording the CBF image, close the scalp with tissue glue and return the animal to the cage.

6.5. Analyze CBF in the selected regions and calculate the CBF recovery percentage compared to contralateral region.

7. Infarct volume measurement by triphenyl tetrazolium chloride (TTC) staining

7.1. Anesthetize the animal with intraperitoneal injection of avertin (250 mg/kg) at 24 h after photothrombosis.

7.2. Perform transcardial perfusion with PBS, collect fresh brain and embed in 3% agar gel.

7.3. Section the brain slice with 1 mm thickness by vibratome and incubate in 2% TTC solution for 10 min.

7.4. Quantify the total infarct volume from 6 brain slices as the absolute volume by ImageJ software.

NOTE: Brain edema was not used as an outcome measurement for two reasons. First, the TTC stain measures tissue viability (via the mitochondrial reduction activity) which is a more severe consequence than edema. Second, as infarction proceeds, both vasogenic and cytotoxic edema occur and cannot be easily distinguished by the standard brain edema measurement methods. However, we have used anti-immunoglobulin (IgG) labeling to assess the integrity of blood-brain-barrier (BBB), and found comparable IgG-extravasation at 6 h after photoactivation in both RB and T+RB stroke models (**Supplementary Figure 3**).

8. Thrombus formation measurement

NOTE: To measure the thrombus formation, collect the brain at 1 h and 2 h after photothrombosis for thrombus measurement in MCA by immunochemistry (IHC) and for fibrin measurement in brain hemisphere by immunoblot, respectively.

8.1. Perform the IHC for the characterization of clot composition. Fix the brain with 4% paraformaldehyde overnight and then dehydrate the brain with 30% sucrose for the OCT embedding.

8.2. Section the brain with sagittal orientation in 20 μ m thickness, and perform the IHC with specific antibodies against fibrinogen, platelet (glycoprotein IIb), red blood cell (TER119) and blood vessel (isolectin GS-IB4).

8.3. Perform the measurement of fibrin in brain hemisphere by immunoblot with an antibody against fibrinogen.

REPRESENTATIVE RESULTS:

First, we compared the fibrin content in RB versus T+RB photothrombosis-induced blood clots. Mice were sacrificed by transcardial perfusion of fixatives at 2 h after photoactivation, and brains were removed for immunofluorescence staining of the MCA branch in longitudinal and transverse planes. In RB photothrombosis, the MCA branch was densely packed with CD41⁺ platelets and little fibrin (**Figure 2A, C**). In contrast, the MCA branch in T+RB photothrombosis was occluded by randomly mixed platelet:fibrin clots (**Figure 2B, D**, $n>3$ for each). We also used immunoblots to compare the fibrin(ogen) level in the cerebral cortex between the two models, after transcardial perfusion with saline at 2 h post-photoactivation. This analysis showed > two-fold increase of fibrin deposition in the ipsilateral hemisphere in T+RB than RB photothrombosis (**Figure 2E**, $p=0.027$ by unpaired *t*-test; $n=3$ for each group). In our original report, we also used confocal microscope-based single vessel photoactivation and intravital imaging to compare the behaviors of FITC-conjugated anti-GP1b β -labeled platelets.²³ Those experiments showed that intravenous injection of 80 U/kg thrombin failed to induce platelet aggregates even under laser illumination (**Figure 3A**), and that platelets form homogenous clots in the RB photothrombosis model (**Figure 3B**), but uneven aggregates with multiple faint regions in T+RB photothrombosis (**Figure 3C**). These results suggest that T+RB photothrombosis increases the fibrin content in the ensuing thrombi.

Next, we compared the effects of acute intravenous tPA treatment (10 mg/kg Alteplase, 30 min after photoactivation) on cerebral blood flow (CBF) recovery between the two models. The CBF of the same mouse at pre- and 24 h post- tPA-versus-vehicle treatment was measured by laser speckle contrast imaging and normalized to the contralateral hemisphere (**Figure 4A, B**). In RB photothrombosis, the tPA treatment led to a trend of CBF-recovery, particularly in the ischemic border area, when compared to vehicle-treated mice (**Figure 4C**, vehicle $51\pm 9\%$ vs tPA $65\pm 7\%$, $p=0.3$ by unpaired *t*-test, $n=4$ for each). In T+RB photothrombosis, the recovery of CBF in tPA-treated mice was more prominent, and the proximal MCA branches often became visible at 24 h (**Figure 4D**, vehicle $55\pm 3\%$ vs tPA $81\pm 7\%$, $p=0.02$ by unpaired *t*-test, $n=6$ for each group). These results suggest greater sensitivity to tPA-lytic therapy by T+RB than RB photothrombosis.

Finally, we used TTC stain to quantify the effects of tPA treatment on infarct size in the RB and T+RB photothrombotic stroke models. In RB photothrombosis, a similar infarct size was detected in vehicle-treated ($18 \pm 2.80 \text{ mm}^3$, $n=6$) and tPA-treated mice ($18 \pm 1.95 \text{ mm}^3$, $n=10$; 10 mg/kg tPA was injected at 30 min post-photoactivation) (**Figure 5A**). In contrast, the tPA-lytic treatment significantly reduced infarction when tPA was injected at 0.5 h ($7 \pm 2.1 \text{ mm}^3$, $n=9$), 1 h ($4.6 \pm 1 \text{ mm}^3$, $n=10$), or 2 h ($6.4 \pm 1.5 \text{ mm}^3$, $n=8$), but not at 6 h post-photoactivation ($15.2 \pm 3.1 \text{ mm}^3$, $n=7$), compared to vehicle-treated mice ($14.8 \pm 2 \text{ mm}^3$, $n=19$) (**Figure 5B**, the p-value determined by unpaired *t*-test). These results indicate that the T+RB photothrombotic stroke model has sensitivity to tPA-lytic treatment in the.

FIGURE AND TABLE LEGENDS:

Figure 1. Outline of procedures. (A) The flow chart of main surgical procedures in T+RB photothrombotic stroke model. Ligation of the ipsilateral common carotid artery (CCA) is optional, but we found it makes the infarct size more consistent, presumably owing to decreased collateral circulation. (B) Top and lateral view of the mouse brain in relationship to skull. Also indicated are the eyes, ear, temporalis muscle, the middle cerebral artery (MCA) and branches, coronal suture, and the laser illumination site. (C) Visualization of the targeted MCA branch underneath the thinned skull (C1) and during laser illumination (C2), and cessation of blood flow after photoactivation (C3). Note the relationship of the MCA branch to the coronal suture. (D) The set-up of a mouse during laser illumination on the left MCA branch.

Figure 2. Different fibrin contents in the blood clots. (A-D) Immunofluorescence labeling of the RB and T+RB photothrombosis-induced thrombi in the distal MCA branch in an either longitudinal (A, B) or transverse plane (C, D) using anti-fibrin (green), anti-CD41/platelet (red), and isolectin B4/endothelial cell (blue) markers. Note the marked increase of anti-fibrin immunosignals in the T+RB photothrombosis-induced blood clots (B, D, $n=3$ for each group). (E) Immunoblotting indicated greater fibrin deposition in ipsilateral cerebral cortex in T+RB than RB photothrombosis at 2 h post-photoactivation ($n=3$ for each). UN: uninjured mice; Cont: contralateral cortex; Ipsi: ipsilateral cortex. Scale bar: 50 μm . This figure is modified with permission from [23].

Figure 3. Intravital imaging of the platelet responses. Confocal microscope-based intravital imaging of FITC-conjugated anti-GP1b β -labeled platelets under single-vessel laser illumination (at the site indicated by white arrows). The experimental groups are: (A) thrombin alone, (B) Rose Bengal alone, and (C) thrombin plus Rose Bengal. The times after laser illumination are labeled. See the video in the JoVE website for this manuscript. Scale bar: 50 μm . This figure is modified with permission from [23].

Figure 4. Effects of tPA-treatment on CBF recovery. Recombinant human tPA (Alteplase, 10 mg/kg) or vehicle was administered via tail vein to RB and T+RB photothrombosis-challenged mouse at 30 min post-laser illumination, and cerebral blood flow (CBF) at pre- and 24 h post-treatment in the same mouse were compared with laser speckle contrast imaging. The CBF in a 3 x 4.8 mm area on both hemispheres was measured. The experimental groups are: (A, C) RB photothrombosis; (B, D) T+RB photothrombosis. Note the significant recovery of CBF by tPA

treatment in the T+RB photothrombosis group ($p=0.02$ by unpaired t-test, $n=4$ for vehicle and $n=6$ for tPA-treatment) and frequent visualization of the proximal MCA branch. In RB photothrombosis, the tPA treatment led to a trend of better CBF, predominantly at the peripheral ischemic area ($p=0.3$ by unpaired t-test, $n=4$ for vehicle and $n=5$ for tPA-treatment). White arrows indicate the site of MCA-photoactivation. This figure is modified with permission from [23].

Figure 5. Effects of tPA-treatment on the infarct size. (A) Intravenous tPA treatment (Alteplase, 10 mg/kg) at 30 min after RB photothrombosis failed to reduce the infarct size ($n=6$ in vehicle-treated and $n=10$ in tPA-treated mice). (B) In contrast, in T+RB photothrombosis, intravenous 10 mg/kg Alteplase treatment at either 0.5, 1, or 2 h, but not at 6 h post-photoactivation led to significant reduction of the infarct size. The p-value was determined by one-way ANOVA with Tukey's multiple comparisons test. This figure is modified with permission from [23].

Table 1: Comparison of selected preclinical stroke models. Filled boxes indicate positivity (the presence of blood clots, platelets, and fibrin) or significant tPA reactivity.

Supplementary Figure 1. CBF monitor after retro-orbital injection of thrombin. (A) The representative photos of retro-orbital sinus (upper panel) and blood flow by laser speckle contrast imaging (lower panel). The three vascular sites (1~3 as labeled) was monitored after thrombin injection (80 U/ kg) into the retro-orbital sinus. (B) The representative tracing graph of blood flow for 15 min after thrombin injection (arrow). (C) The laser speckle-based quantification showed no reduction of blood flow near the retro-orbital sinus within 15 min after thrombin injection ($n=4$, p-value determined by unpaired t-test).

Supplementary Figure 2. Lack of fibrin deposition in contralateral hemisphere at 6 hours after photoactivation. Immunostaining of the anti-fibrinogen (green) showed fibrin deposition in the ipsilateral cortex at 6 h after RB and T+RB photothrombosis. In contrast, there was no discernible fibrin deposition in the contralateral cortex following thrombin-enhanced photothrombosis. $N=4$ for each group. Scale bar: 50 μm . Blue fluorescence as the DAPI-nucleus staining.

Supplementary Figure 3. Lack of immunoglobulin (IgG) extravasation after photothrombosis. At 6 h after unilateral MCA-targeted photoactivation, immunostaining showed extravasation of IgG in the ipsilateral hemisphere, but not in contralateral hemisphere, suggesting restricted BBB damage after thrombin-enhanced photothrombosis. $N=4$ for each. Scale bar: 50 μm .

DISCUSSION:

The traditional RB photothrombotic stroke, introduced in 1985, is an attractive model of focal cerebral ischemia for simple surgical procedures, low mortality, and high reproducibility of brain infarction.⁵ In this model, the photodynamic dye RB rapidly activates platelets upon light excitation, leading to dense aggregates that occlude the blood vessel^{5,8,23}. However, the small amount of fibrin in RB-induced blood clots (Figure 2) deviates from the dominant platelet:fibrin intermixed pattern of thrombi retrieved acutely in ischemic stroke patients^{21,22}. The low fibrin content in RB-induced thrombi likely also contributes to its resilience to tPA-lytic treatment^{7,8,19}.

Though ultraviolet laser irradiation induces vascular recanalization in RB photothrombosis, this experimental therapy is unlikely to be used clinically⁷. Thus, the traditional RB photothrombotic stroke has been mainly used as a permanent occlusion model, less suited for thrombolysis and neuroprotection research (the latter often uses intraluminal suture MCAO model that features rapid vascular reperfusion upon removal of the mechanical occlusion).

We hypothesized that using admixture of RB and a sub-thrombotic dose of thrombin for photoactivation may increase the fibrin content in ensuing thrombi and enhance the responses to tPA thrombolysis, the real-world stroke therapy. This hypothesis is supported by the results presented here and in our original report.²³ The thrombin-enhanced photothrombotic stroke model also maintains the advantages of low mortality, simple surgical procedures, and high consistency in infarction size and location, as in traditional RB photothrombosis model. Hence, we believe that thrombin-enhanced photothrombosis is a valuable addition to the repertoire of thromboembolic stroke models (**Table 1**). Two procedural details of the thrombin-enhanced photothrombosis model warrants discussion. First, over-dose of intravenous thrombin may provoke acute pulmonary thromboembolism and animal mortality²⁵. We examined a range of thrombin doses for combination with RB photothrombosis, and the chosen 80 U/kg dose has not induced mortality in >100 experimented adult male C57Bl/6 mice so far. It is likely that the thrombin dose needs adjustment for mice with hypercoagulation states²⁶. Second, we routinely ligated the ipsilateral CCA besides MCA-targeted photothrombosis in our procedures. We found that ligation of the ipsilateral CCA further increases the consistency in infarct size, which may be due to diminished collateral circulation between MCA and the anterior plus posterior cerebral arteries.

With its unique properties, the thrombin-enhanced photothrombotic stroke model may be particularly useful for at least three research topics. First, this new model is ideally suited for head-to-head comparison of tPA and other fibrinolytic agents such as Tenecteplase (TNKase)²⁷. TNKase is an engineered tPA-mutant variant with increased fibrin-specificity and a lower risk for iatrogenic hemorrhage in ex vivo experiments. Yet, its superiority to tPA has only been tested in a micro-embolic stroke model and using a binary neurological outcome analysis¹⁴. Given its high reproducibility and quantitative infarct size analysis, the thrombin-enhanced photothrombotic stroke model can be used to compare the benefits and adverse effects of tPA-versus-TNKase in multiple aspects (e.g., dose responses, therapeutic window, comorbidity impacts, and potential adverse effects in delayed treatment). Second, the thrombin-enhanced photothrombosis model may be useful for investigating the effects of combined tPA and anti-platelet treatment in acute ischemic stroke²⁸. Recent advances of endovascular procedures in ischemic stroke have enabled researchers to analyze the histological composition of acute thrombi and identified a dominant, intermixed platelet:fibrin pattern^{21,22}. Accordingly, the combination of a fibrinolytic agent (tPA) and anti-platelet agents may boost the overall efficacy of thrombolysis, but a stroke model that simulate the clinical platelet:fibrin composition of thrombus is crucial for such research. Along with the tHI and emboli-MCAO models, thrombin-photothrombosis meets this requirement and stands out for its low mortality, simple surgical procedures, and lack of systemic cardiovascular effects (**Table 1**).

Last but not least, thrombin-enhanced photothrombosis may be particularly useful for investigating stroke-induced collateral circulation, given its predictable peri-infarct location in the MCA-supplying territory. By sustaining the penumbra to offset infarct growth, collateral circulation is increasingly recognized as an important predictor of ischemic stroke outcomes, because acute vascular obstruction promotes blood flow across collateral network, followed by remodeling and angiogenesis to form neo-collateral vessels^{29,30}. The results suggest that tPA not only promotes recanalization of the proximal MCA, but also increases collateral circulation in the peripheral of MCA-supplying area (**Figure 4**). Better understanding the mechanisms that regulates the plasticity of collateral circulation may suggest novel therapies. As the thrombin-enhanced photothrombotic stroke model offers the advantage of predictable peri-infarct region and sensitivity to lytic treatment, it will assist the research of post-stroke collateral circulation.

ACKNOWLEDGMENTS:

This work was supported by the NIH grants (NS108763, NS100419, NS095064, and HD080429 to C.-Y. K.; and NS106592 to Y.-Y.S.).

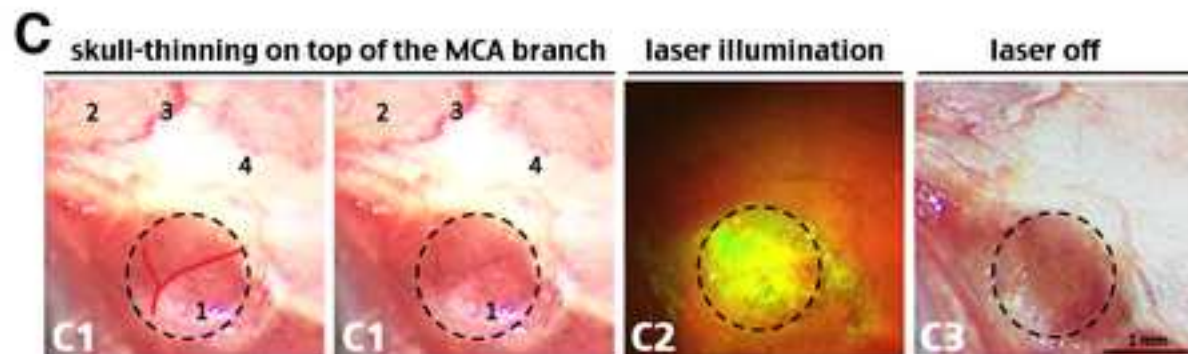
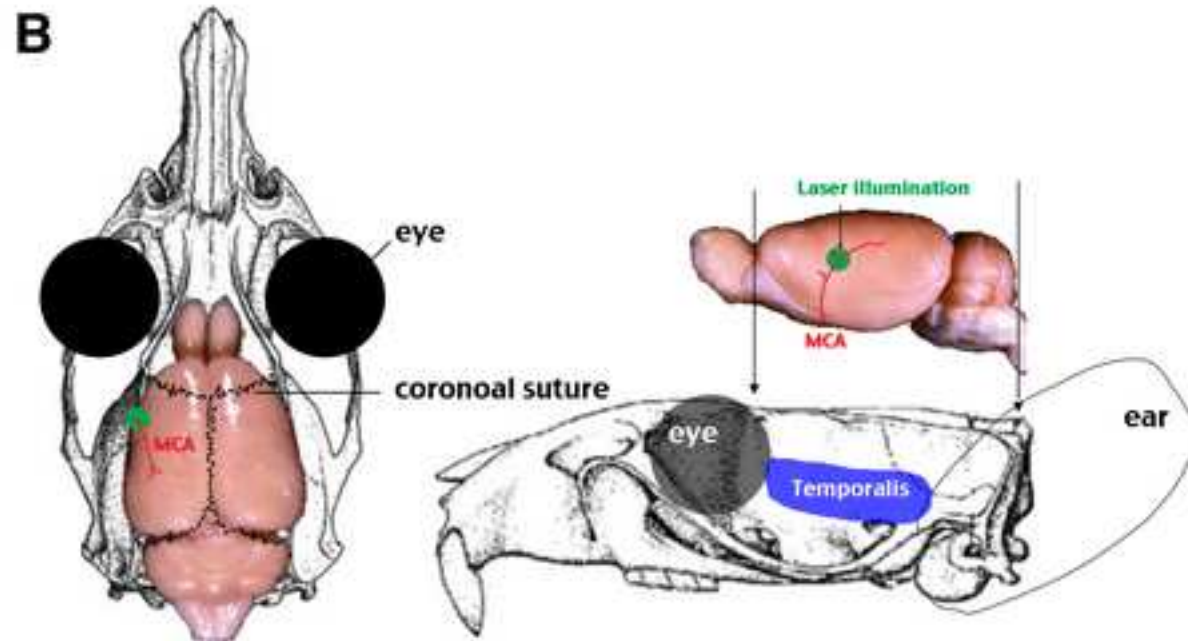
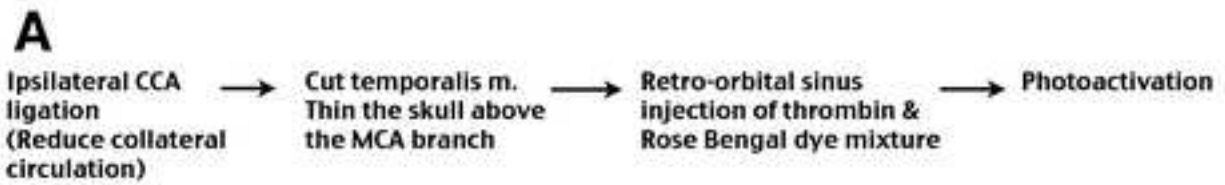
DISCLOSURES:

The authors have nothing to disclose

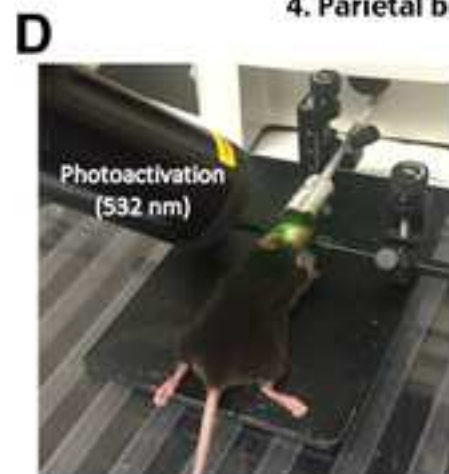
REFERENCES:

1. Lyden, P.D. *Thrombolytic Therapy for Acute Stroke*. 3/e, Springer (2015).
2. Linfante, I., Cipolla, M.J. Improving reperfusion therapies in the era of mechanical thrombectomy. *Translational Stroke Research*. **7** (4), 294-302 (2016).
3. Campbell, B.C. et al. Endovascular Therapy for Ischemic stroke with perfusion-imaging selection. *The New England Journal of Medicine*. **372** (11), 1009-1018 (2015).
4. Hossmann K.A. The two pathophysiologicals of focal brain ischemia: implications for translational stroke research. *Journal of Cerebral Blood Flow and Metabolism*. **32** (7), 1310-1316 (2012).
5. Longa, E.Z., Weinstein, P.R., Carlson, S., Cummins, R. Reversible middle cerebral artery occlusion without craniectomy in rats. *Stroke*. **20** (1), 84-91 (1989).
6. Watson, B.D., Dietrich, W.D., Busto, R., Wachtel, M.S., Ginsberg, M.D. Induction of reproducible brain infarction by photochemically initiated thrombosis. *Annals of Neurology*. **17** (5), 497-504 (1985).
7. Watson, B.D., Prado, R., Veloso, A., Brunschwig, J.P., Dietrich, W.D. Cerebral blood flow restoration and reperfusion injury after ultraviolet laser-facilitated middle cerebral artery recanalization in rat thrombotic stroke. *Stroke*. **33** (2), 428-434 (2002).
8. Uzdensky, A.B. Photothrombotic stroke as a model of ischemic stroke. *Translational Stroke Research*. **9** (5), 437-451 (2018).
9. Karatas, H. et al. Thrombotic distal middle cerebral artery occlusion produced by topical FeCl(3) application: a novel model suitable for intravital microscopy and thrombolysis studies. *Journal of Cerebral Blood Flow and Metabolism*. **31** (6), 1452-1460 (2011).
10. Orset, C. et al. Mouse model of in situ thromboembolic stroke and reperfusion. *Stroke*. **38** (10), 2771-2778 (2007).

11. Orset, C. et al. Efficacy of Alteplase in a mouse model of acute ischemic stroke: A retrospective pooled analysis. *Stroke*. **47** (5), 1312-1318 (2016).
12. Kudo, M., Aoyama, A., Ichimori, S., Fukunaga, N. An animal model of cerebral infarction. Homologous blood clot emboli in rats. *Stroke*. **13** (4), 505-508 (1982).
13. Busch, E., Kruger, K., Hossmann, K.A. Improved model of thromboembolic stroke and rt-PA induced reperfusion in the rat. *Brain Research*. **778** (1), 16-24 (1997).
14. Lapchak, P.A., Araujo, D.M., Zivin, J.A. Comparison of Tenecteplase with Alteplase on clinical rating scores following small clot embolic strokes in rabbits. *Experimental Neurology*. **185** (1), 154-159 (2004).
15. Sun, Y.Y. et al. Synergy of combined tPA-Edaravone therapy in experimental thrombotic stroke. *PLoS One*. **9** (6), e98807 (2014).
16. Sun, Y.Y. et al. Prophylactic Edaravone prevents transient hypoxic-ischemic brain injury: Implications for perioperative neuroprotection. *Stroke*. **46** (7), 1947-1955 (2015).
17. Sun, Y.Y. et al. Sickie mice are sensitive to hypoxia/ischemia-induced stroke but respond to tissue-type plasminogen activator treatment. *Stroke*. **48** (12), 3347-3355 (2017).
18. Sun, Y.Y., Kuan, C.Y. A thrombotic stroke model based on transient cerebral hypoxia-ischemia. *Journal of Visualized Experiments*. (102), e52978 (2015).
19. Pena-Martinez, C. et al. Pharmacological modulation of neutrophil extracellular traps reverses thrombotic stroke tPA (tissue-type plasminogen activator) resistance. *Stroke*. **50** (11), 3228-3237 (2019).
20. Denorme, F. et al. ADAMTS13-mediated thrombolysis of t-PA-resistant occlusions in ischemic stroke in mice. *Blood*. **127** (19), 2337-2345 (2016).
21. Marder, V.J. et al. Analysis of thrombi retrieved from cerebral arteries of patients with acute ischemic stroke. *Stroke*. **37** (8), 2086-2093 (2006).
22. Bacigaluppi, M., Semerano, A., Gullotta, G.S., Strambo, D. Insights from thrombi retrieved in stroke due to large vessel occlusion. *Journal of Cerebral Blood Flow and Metabolism*. **39** (8), 1433-1451 (2019).
23. Sun, Y.Y. et al. A murine photothrombotic stroke model with an increased fibrin content and improved responses to tPA-lytic treatment. *Blood Advances*. **4** (7), 1222-1231 (2020).
24. Su, E.J. et al. Activation of PDGF-CC by tissue plasminogen activator impairs blood-brain barrier integrity during ischemic stroke. *Nature Medicine*. **14** (7), 731-737 (2008).
25. Gupta, A.K. et al. Protective effects of gelsolin in acute pulmonary thromboembolism and thrombosis in the carotid artery of mice. *PLoS One*. **14** (4), e0215717 (2019).
26. Carroll, B.J., Piazza, G. Hypercoagulable states in arterial and venous thrombosis: When, how, and who to test? *Vascular Medicine*. **23** (4), 388-399 (2018).
27. Coutts, S.B., Berge, E., Campbell, B.C., Muir, K.W., Parsons, M.W. Tenecteplase for the treatment of acute ischemic stroke: A review of completed and ongoing randomized controlled trials. *International Journal of Stroke*. **13** (9), 885-892 (2018).
28. McFadyen, J.D., Schaff, M., Peter, K. Current and future antiplatelet therapies: emphasis on preserving haemostasis. *Nature Reviews Cardiology*. **15** (3), 181-191 (2018).
29. Bang, O.Y., Goyal, M., Liebeskind, D.S. Collateral circulation in ischemic stroke: Assessment tools and therapeutic strategies. *Stroke*. **46** (11), 3302-3309 (2015).
30. Faber, J.E., Chilian, W.M., Deindl, E., van Royen, N., Simons, M. A brief etymology of the collateral circulation. *Arteriosclerosis, Thrombosis, Vascular Biology*. **34** (9), 1854-1859 (2014).



- (MCA added)
1. Proximal MCA branch
 2. Frontal bone
 3. Coronal suture
 4. Parietal bone



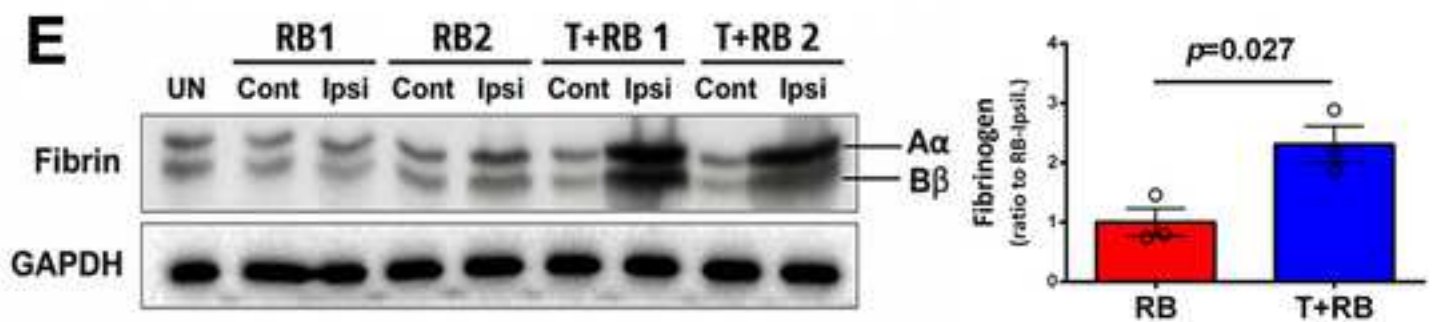
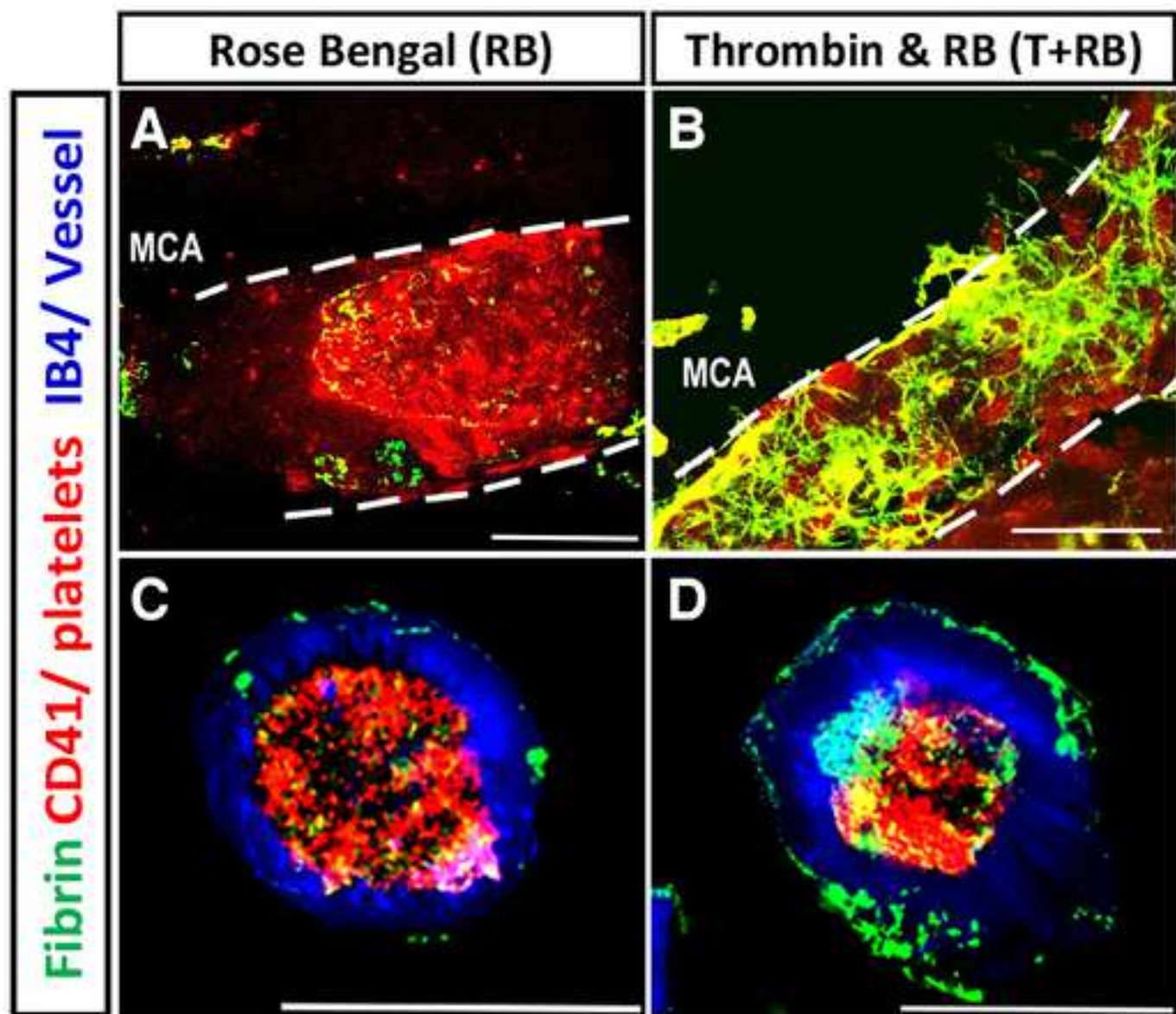
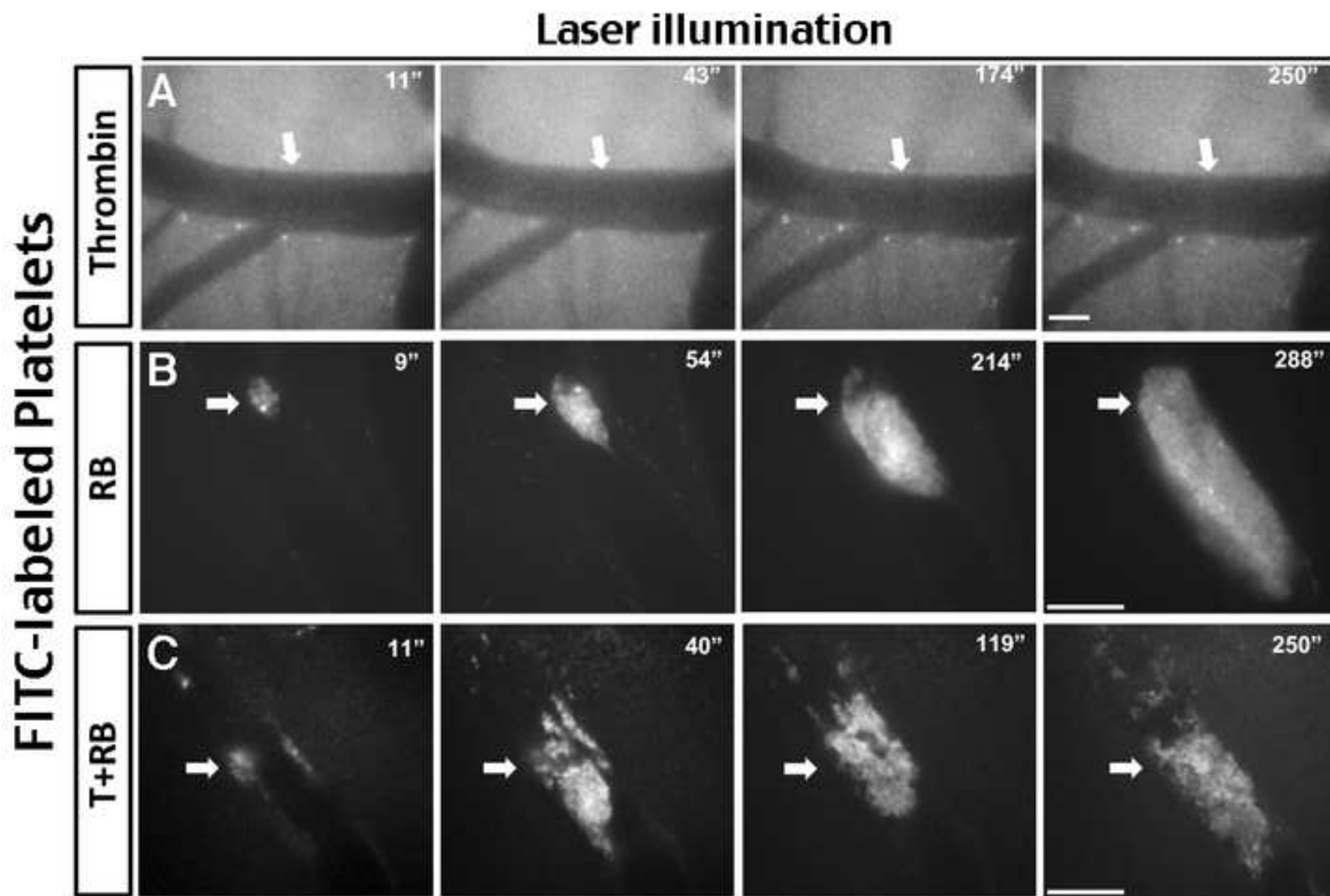
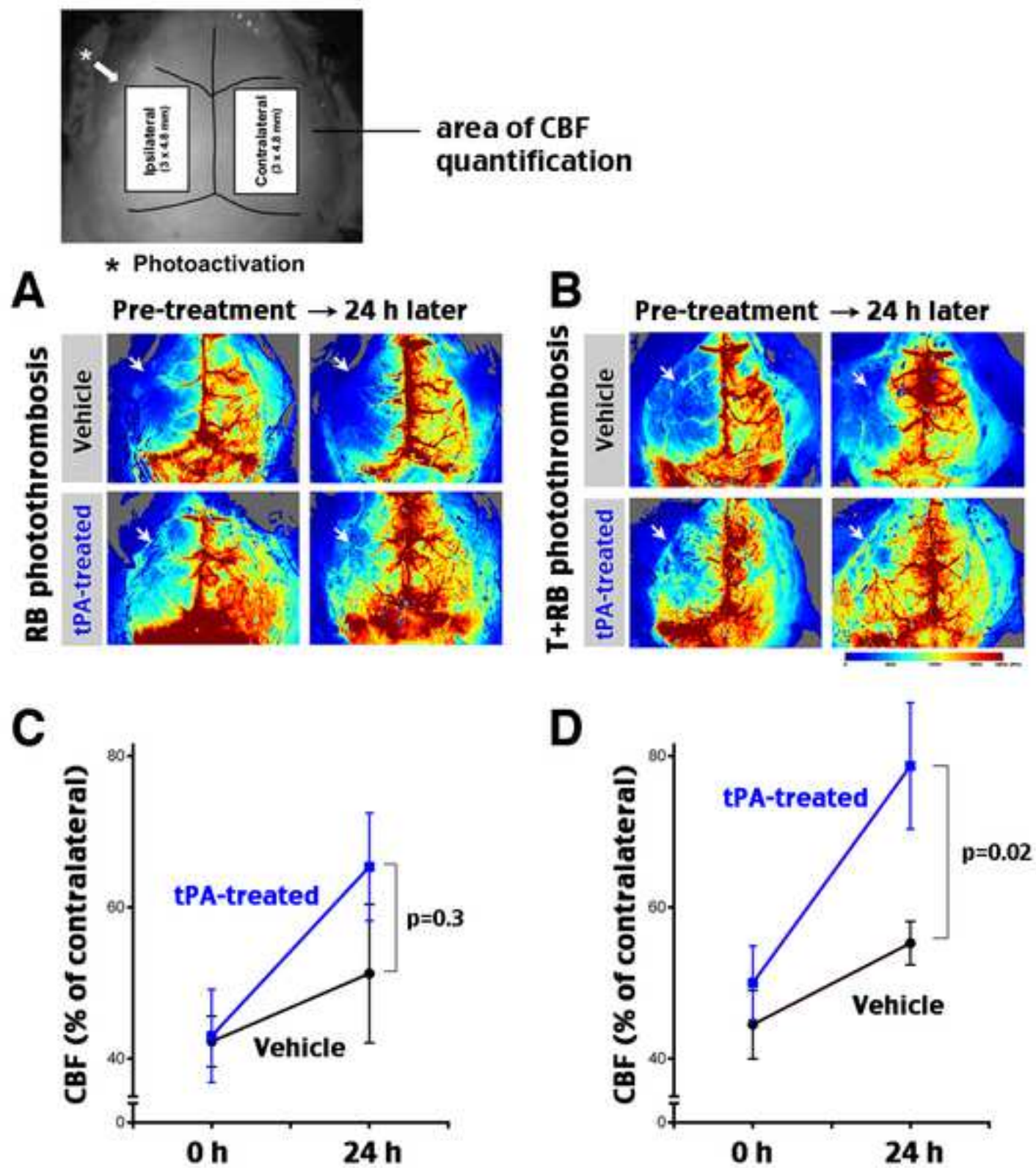


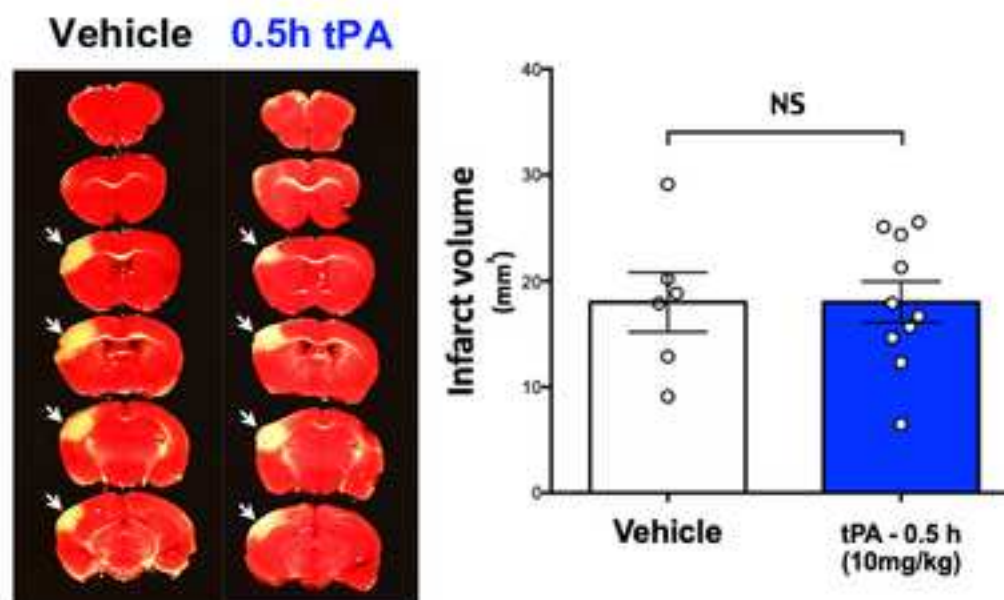
Figure 3. Intravital imaging of the platelet responses.

[Click here to access/download;Figure;Figure3.tif](#)

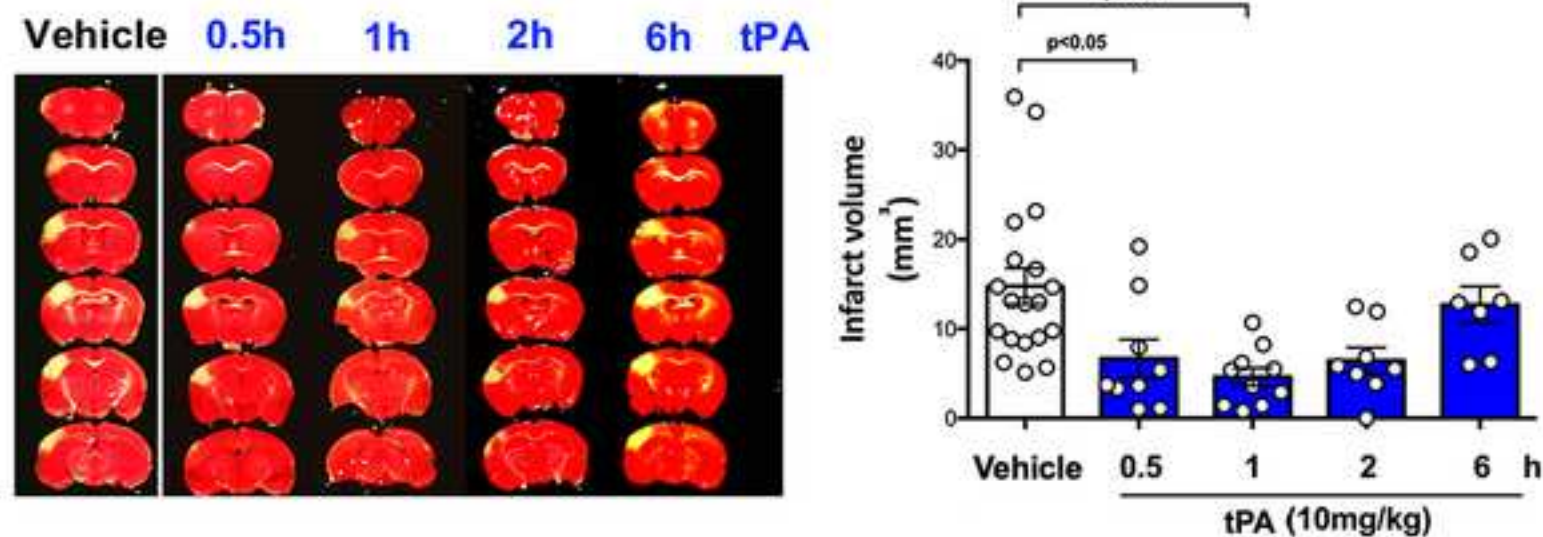


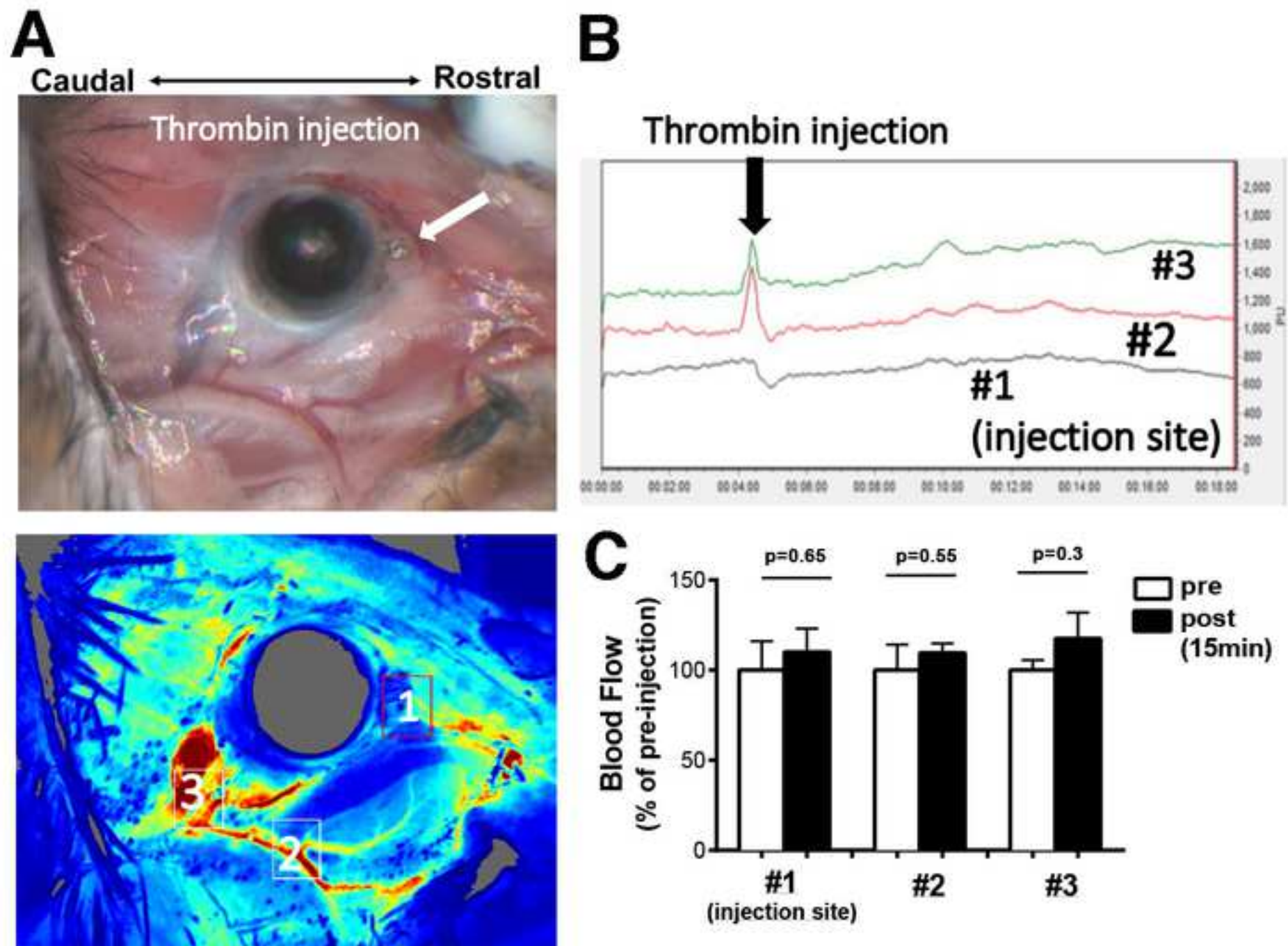


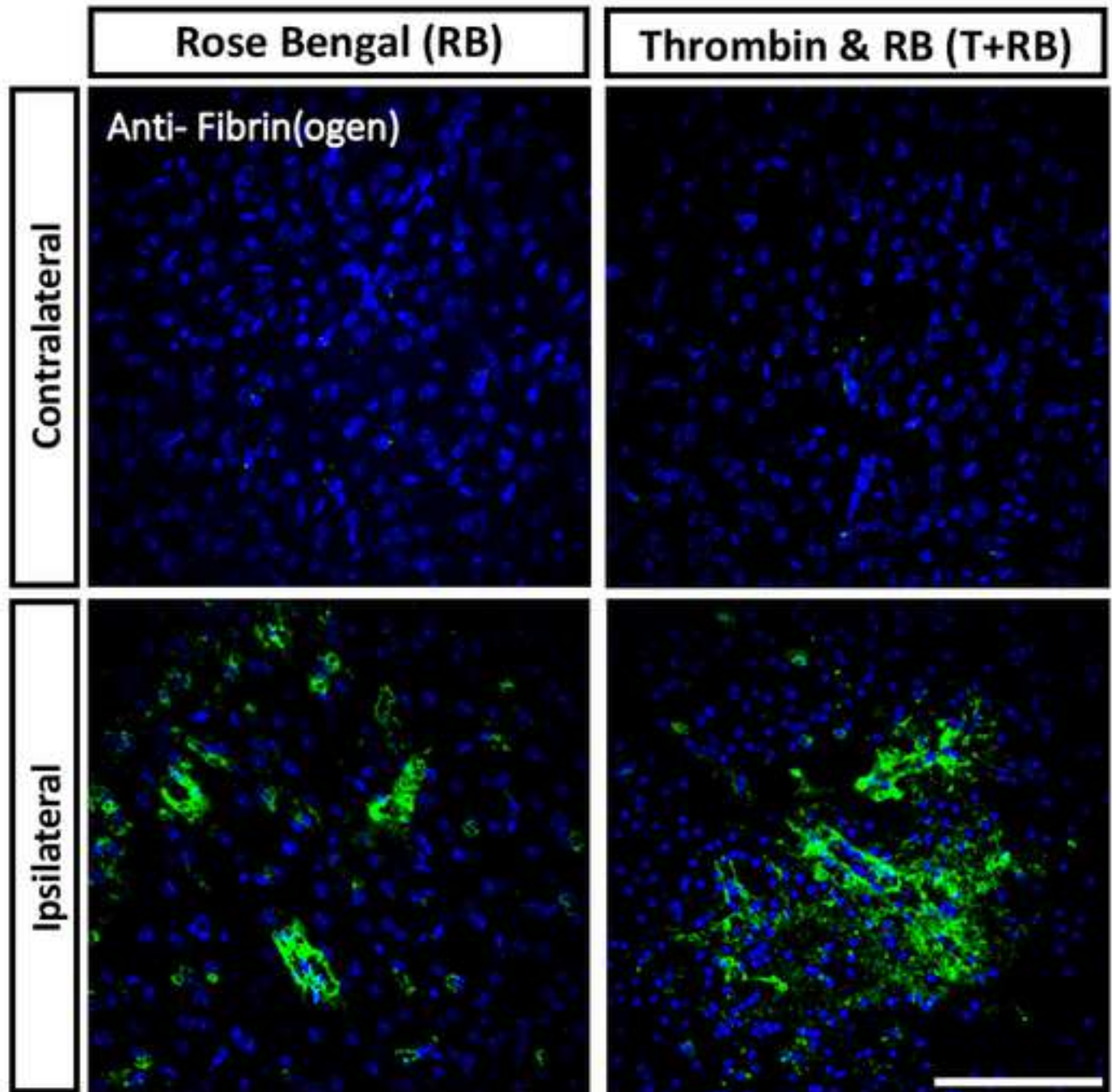
A RB Phtothrombosis

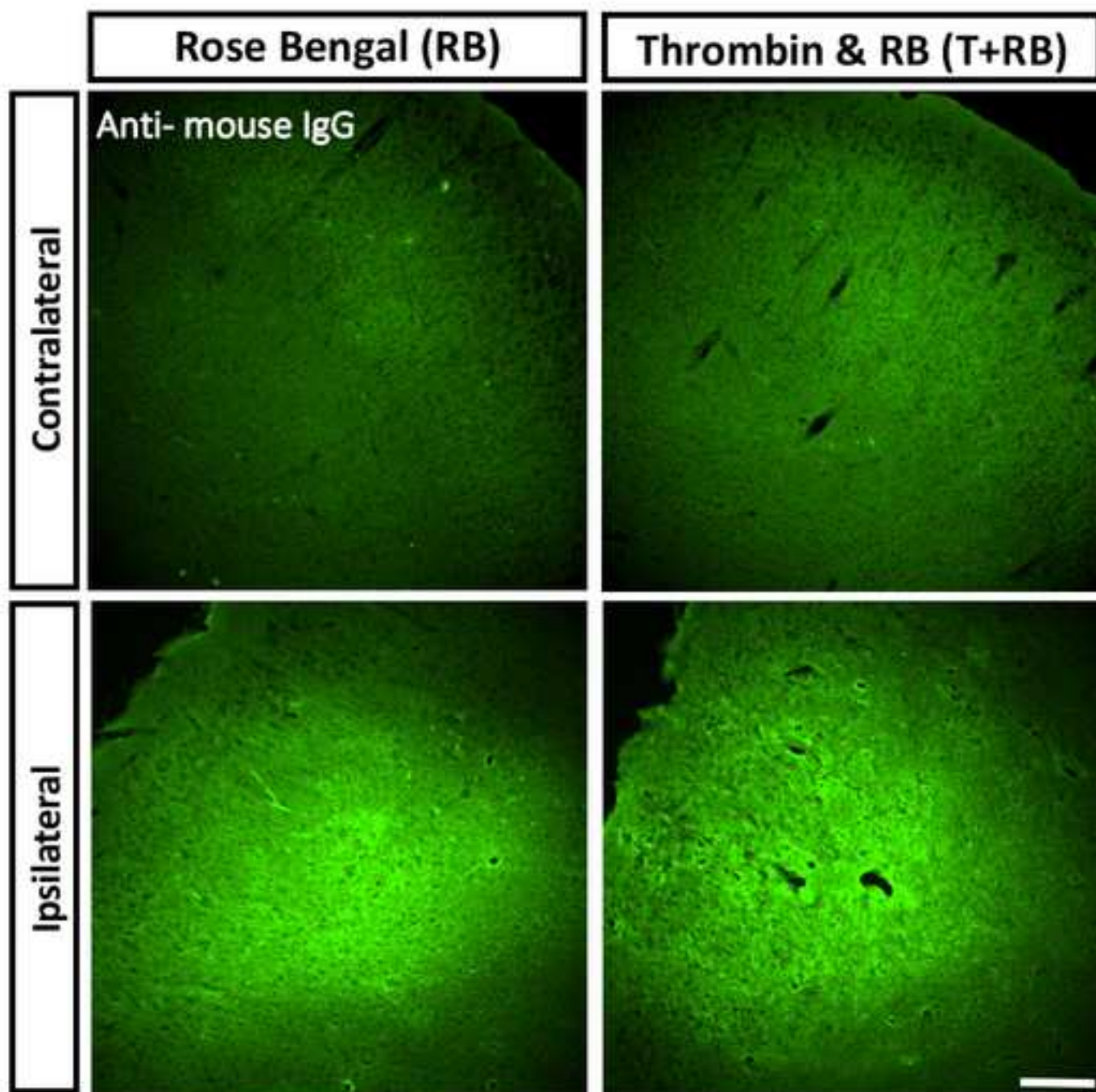


B T+RB Phtothrombosis









Model	Surgical Procedure	Blood clots	Platelets	Fibrin	tPA-reactivity
Intraluminal suture MCAO	Endovascular MCA occlusion	No	N/A	N/A	No
Photothrombosis	Skull thinning and photoactivation	Yes			Weak
Thrombin-Photothrombosis	UCCA0, Skull thinning and photoactivation	Yes			Yes
FeCl ₃ (on the MCA)	Skull thinning and chemical activation	Yes			No
in situ thrombin injection	Craniotomy and MCA microinjection	Yes			Yes
Emboli-MCAO	Endovascular MCA occlusion	Yes			Yes
Transient Hypoxia-Ischemia (tHI)	UCCA0 plus hypoxia	Yes			Yes

Main features/utility

Rapid reperfusion; Neuroprotection study; tPA-induced BBB injury
High reproducibility; low mortality
High reproducibility; low mortality
High reproducibility; low mortality
High reproducibility; low mortality; tPA-lytic treatment
tPA-lytic treatment; Variable clot hardness
Infarct > the MCA area; Systemic CV effects

Key references

Longa et al. 1989 (Ref #5)
Watson et al. 1985 (Ref #6)
Sun et al. 2020 (Ref #23)
Karatas et al. 2011 (Ref #69)
Orset et al. 2007 (Ref #10)
Busch et al. 1997 (Ref #13)
Sun et al. 2014 (Ref #15)

Name	Company	Catalog Number	Comments
2,3,5-triphenyltetrazolium chloride (TTC)	Sigma	T8877	infarct
4-0 Nylon monofilament suture	LOOK	766B	surgical supplies
5-0 silk suture	Harvard Apparatus	624143	surgical supplies
543nm laser beam	Melles Griot	25-LGP-193-249	photothrombosis
adult male mice	Charles River	C57BL/6	10~14 weeks old (22~30 g)
Anesthesia bar for mouse adaptor	machine shop, UVA		surgical setup
Avertin (2, 2, 2-Tribromoethanol)	Sigma	T48402	euthanasia
Dental drill	Dentamerica	Rotex 782	surgical setup
Digital microscope	Dino-Lite	AM2111	brain imaging
Dissecting microscope	Olympus	SZ40	surgical setup
Fine curved forceps (serrated)	FST	11370-31	surgical instrument
Fine curved forceps (smooth)	FST	11373-12	surgical instrument
goat anti-rabbit Alexa Fluor 488	Invitrogen	A11008	Immunohistochemistry
Halsted-Mosquito hemostats	FST	13008-12	surgical instrument
Heat pump with warming pad	Gaymar	TP700	surgical setup
infusion pump	KD Scientific	200	thrombolytic treatment
Insulin syringe with 31G needle	BD	328291	photothrombosis
Ketamine	CCM, UVA		anesthesia
Laser protective google 532nm	Thorlabs	LG3	photothrombosis
Meloxicam SR	CCM, UVA		NSAID analgesia
micro needle holders	FST	12060-01	surgical instrument
micro scissors	FST	15000-03	surgical instrument
MoorFLPI-2 blood flow imager	Moor	780-nm laser source	Laser Speckle Contrast Imaging
Mouse adaptor	RWD	68014	surgical setup
Puralube Vet ointment	Fisher	NC0138063	eye dryness prevention
Retractor tips	Kent Scientific	Surgi-5014-2	surgical setup
Rose Bengal	Sigma	198250	photothrombosis
Thrombin	Sigma	T7513	photothrombosis
Tissue glue	Abbott Laboratories	NC9855218	surgical supplies
tPA	Genetech	Cathflo activase 2mg	thrombolytic treatment
Vibratome	Stoelting	51425	TTC infarct
Xylazine	CCM, UVA		anesthesia

MS# JoVE61740**Authors' Responses to Comments**

We thank the editorial and reviewers' positive comments of our manuscript very much, and appreciate the opportunity to introduce our novel stroke model at The Journal of Visualized Experiments (JoVE). Both reviewers found our stroke model interesting and useful, and provided very constructive comments to improve our manuscript. We have performed new experiments or added information to the revised manuscripts. These major changes are indicated in blue-color fonts. Since the JoVE papers are procedure-oriented, we chose to describe several supplementary results as **Note** in the manuscript, while providing the experimental data for reviewers' perusal in this document. Further, we have highlighted the key experimental procedures to be filmed for the video component of publication in response to the editor's request. The following is a point-by-point summary of our responses to the editor's and both reviewers' comments.

Editorial comments

1. Please take this opportunity to thoroughly proofread the manuscript to ensure that there are no spelling or grammatical errors.

Thanks for the reminder. We have carefully proofread the manuscript and slightly edited the text for clarity and /or brevity.

2. Please include at least 6 keywords/phrases.

One keyword, **thrombolysis**, is added to make the number of keywords/phrases to be 6.

3. Protocol Language: Please ensure that all text in the protocol section is written in the imperative voice/tense as if you are telling someone how to do the technique (i.e. "Do this", "Measure that" etc.) Any text that cannot be written in the imperative tense may be added as a "Note", however, notes should be used sparingly and actions should be described in the imperative tense wherever possible. Examples NOT in the imperative: 1.2, 2.6

We have edited the procedures to be in an imperative/command voice, as suggested.

4. Protocol Detail: Please note that your protocol will be used to generate the script for the video, and must contain everything that you would like shown in the video. Currently, the protocol seems incomplete.

1) 3.4: mention drill speed. We have added "burr speed setting at 50% of speed controller".

2) 3.8: do you mean 0.5 mW? Yes, we have added "with 0.5 mW energy".

3) 4.2: what is done after this? How are the effects of tPA treatment evaluated? Is any imaging performed? How are the animals handled? How was cerebral blood flow monitored? Describe the steps involved in laser speckle imaging briefly. To evaluate the effect of tPA treatment, the CBF monitor or infarct volume measurement (TTC staining) is applied. Those procedures are added as "step 6) Monitoring the cerebral blood flow (CBF)" and "step 7) Analysis of the infarct size by triphenyl tetrazolium chloride (TTC) staining".

4) Mention blood clot extraction and immunofluorescence staining steps. We have added "step 8) Analysis of the histological composition of thrombi".

5) Mention steps for TTC staining briefly. These are now described in "step 7) Analysis of the infarct size by triphenyl tetrazolium chloride (TTC) staining".

6) When is intravital imaging performed? Please describe the steps, including all settings. The intravital imaging is an optional procedure. We added this optional procedure as "step 4".

5. Protocol Highlight: Please highlight ~2.5 pages or less of text (which includes headings and spaces) in **yellow**, to identify which steps should be visualized to tell the most cohesive story of your protocol steps. **We have highlighted these key steps in yellow for the JoVE staff to prepare the filming script.**

6. Discussion: JoVE articles are focused on the methods and the protocol, thus the discussion should be similarly focused. Please ensure that the discussion covers the following in detail and in paragraph form (3-6 paragraphs): 1) modifications and troubleshooting, 2) limitations of the technique, 3) significance with respect to existing methods, 4) future applications and 5) critical steps within the protocol.

Thanks for the reminder. We have carefully reviewed the Discussion and confirm that it contains all five key components, as suggested by the editor.

7. Commercial Language: JoVE is unable to publish manuscripts containing commercial sounding language, including trademark or registered trademark symbols (TM/R) and the mention of company brand names before an instrument or reagent. Examples of commercial sounding language in your manuscript are Nair and betadine. Please use generic names instead. **Thanks for the reminder. We have edited the manuscript to delete the commercial language, as indicated.**

8. If your figures and tables are original and not published previously or you have already obtained figure permissions, please ignore this comment. If you are re-using figures from a previous publication, you must obtain explicit permission to re-use the figure from the previous publisher (this can be in the form of a letter from an editor or a link to the editorial policies that allows you to re-publish the figure). Please upload the text of the re-print permission (may be copied and pasted from an email/website) as a Word document to the Editorial Manager site in the "Supplemental files (as requested by JoVE)" section. Please also cite the figure appropriately in the figure legend, i.e. Page 3 of 3 "This figure has been modified from [citation]." **We have added "This figure is modified with permission from [23]" in the revised manuscript. Reference [23] is our original paper in Blood Advances. We will also upload the permission for reproduction from the journal into the JoVE on-line submission system.**

Reviewer 1

Manuscript Summary:

The traditional photothrombotic stroke model preferentially induces platelet aggregates that are resistant to tissue plasminogen activator (tPA)-lytic therapy. The authors present a modified photothrombotic model by co-injecting thrombin and photosensitive dye for photoactivation in mice. This thrombin-enhanced photothrombotic model produces mixed platelet/fibrin clots and is highly sensitive to tPA-lytic treatment. **We thank this reviewer for succinct and precise summary of the key features/advantages of our stroke model!**

Major Concerns: Authors inject RB and thrombin into the retro-orbital sinus, however, even though the RB remains unactivated until laser stimulus in the MCA, thrombin starts to generate clot once injected. How do authors control that thrombus formation does not occur in the retro-

orbital sinus? Authors must explain and show data regarding this issue and should include a fibrin control with its corresponding immunohistochemistry of the thrombus content.

We thank this reviewer for this important reminder. We have performed two new experiments to examine this issue. As shown in **Figure 1**, we used laser speckle contrast imaging to monitor the blood flow in three vasculatures near the orbital cavity where we injected 80 U/kg thrombin into the retro-orbital sinus. Shown are the locations of the 3 labeled (1-3) vascular site and their blood flow from 3 min before to 15 min after thrombin-injection. Quantification showed a similar level of blood flow pre- and post-thrombin injection (n=4 mice for experiments). In **Figure 2**, we used anti-fibrin(ogen) immunostaining to compare blood-clotting in RB and T+RB photothrombosis. We found that both stroke models induce fibrin deposits ONLY in the ipsilateral cerebral cortex. These results suggest that the addition of 80 U/kg thrombin in the T+RB photothrombotic stroke model does not induce widespread blood clotting and fibrin deposition. Since the focus of JoVE paper is on the model procedures, we added a Note to step 3.6 to describe these findings and the mortality rate data in our pilot experiments. We stated,

Note: In pilot experiments, we examined the mortality rate of increasing doses of thrombin mixed with the standard dose of RB dye (50 mg/kg) for photoactivation. The mortality was 0% for 80 U/kg thrombin (n=13), 43% for 120 U/kg thrombin (n=7), and 100% for both 160 U/kg (n=5) and 200 U/kg thrombin (n=5). A dose of 80 U/kg thrombin was therefore chosen for this model. We also used laser speckle contract imaging to exclude the possibility of rampant blood clotting near the orbital cavity after retro-orbital sinus injection of T+RB, as well as, widespread fibrin deposition in the contralateral hemisphere that was not subjected to laser illumination (data not shown).

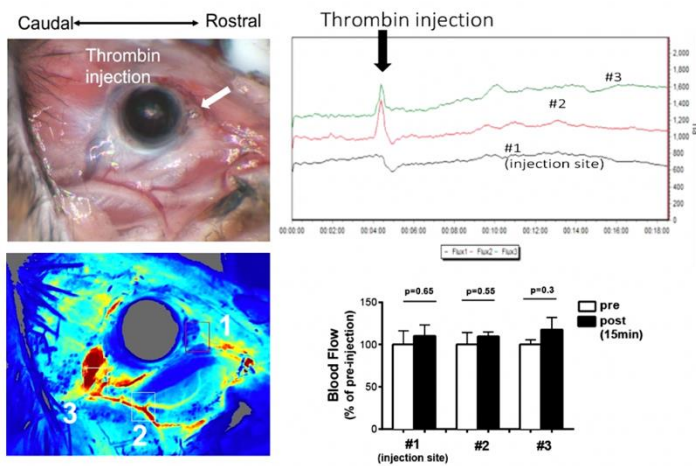


Fig 1. Monitoring the blood flow near the orbital cavity after thrombin injection. Laser speckle contrast imaging was used to track the three vascular sites (1-3, as labeled) after retro-orbital injection of 80 U/kg thrombin. No blood flow reduction was noted at either site (n=4).

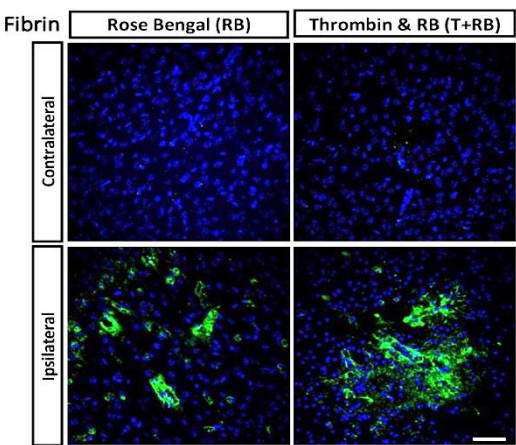


Fig 2. Immunostaining showed the lack of fibrin deposits in contralateral hemisphere in the RB and T+RB photothrombosis model (n=4 each, scale bar: 50 μ m)

Minor Concerns:

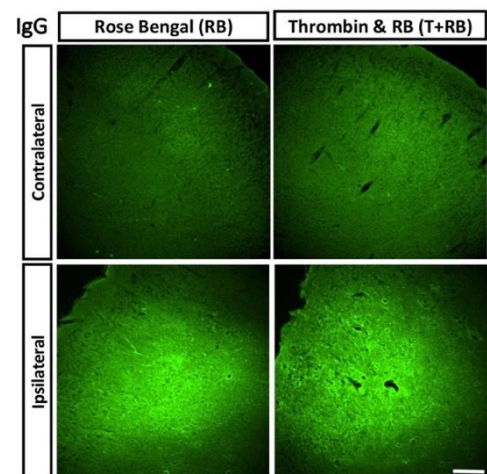
1.Authors inject recombinant human tPA through the tail vein with a 50% bolus and 50% over 30 min by infusion pump. Authors should justify it and include some reference.

We thank for this reminder for clarification. Due to reduced potency of human tPA on murine plasminogen, the vast majority of preclinical stroke research has used the dose of 10 mg/kg and a 50/50 bolus/infusion protocol for intravenous rtPA (Alteplase) administration in rodents, as in Su et al., Nat Med. 2008; 14: 731–737 (PMID 18568034, ref#24). We added a Note to step 5.2.

Note: Although the clinical dose of recombinant human tPA for acute ischemic stroke treatment is 0.9 mg/kg, a higher dose (10 mg/kg) is commonly used in rodents to compensate for reduced cross-species tPA reactivity. We also followed the standard protocol of tPA-administration in preclinical stroke models, using 50% as a bolus and 50% infused through the tail vein over 30 min.²⁴

2. Authors should measure the edema index due to the disruption on endothelial integrity with the PT model (Labatgest & Tomasi, 2013).

We thank for this interesting point. We actually have assessed blood-brain-barrier integrity using anti-IgG staining to examine brains at 6 h post-photoactivation in both RB and T+RB models. As shown in the figure on the right, our experiment showed comparable IgG-leakage prior to infarction in both models. However, we opted not to perform brain edema quantification, because it seems less central to our hypothesis of increased fibrin content in the T+RB-induced photo-thrombotic stroke clots. In the revised manuscript, we added the following Note to step 7.4.



Note: We did not use brain edema as an outcome measurement for two reasons. First, the TTC stain measures tissue viability (via the mitochondrial reduction activity) which is a more severe consequence than edema. Second, as infarction proceeds, both vasogenic and cytotoxic edema occur and cannot be easily distinguished by the standard brain edema measurement methods. However, we have used anti-immunoglobulin (IgG) labeling to assess the integrity of blood-brain-barrier (BBB), and found comparable IgG-extravasation at 6 h after photoactivation in both RB and T+RB stroke models.

Reviewer 2

Manuscript Summary:

The present study aimed to investigate a new model system called the thrombin-enhanced photothrombotic stroke (PTS) model, which produces mixed platelets. This stroke model consists of fibrin clots and is highly sensitive to tPA lytic, and may be a useful tool to develop better thrombolytic therapies. This is an important and useful stroke model. However, there are some minor concerns that need to be addressed. We thank this reviewer for very positive and helpful comments of our manuscript!

Minor Concerns:

1. What is the mortality rate of the thrombi and RB-combined photothrombosis model?

This is indeed an important point. We thank for this reminder, and have added the data in our pilot experiments as a Note to step 3.6. We stated the following:

Note: In pilot experiments, we examined the mortality rate of increasing doses of thrombin mixed with the standard dose of RB dye (50 mg/kg) for photoactivation. The mortality was 0% for 80 U/kg thrombin (n=13), 43% for 120 U/kg thrombin (n=7), and 100% for both 160 U/kg (n=5) and 200 U/kg thrombin (n=5). A dose of 80 U/kg thrombin was therefore chosen for this model. We also used laser speckle contrast imaging to exclude the possibility of rampant blood clotting near the orbital cavity after retro-orbital sinus injection of T+RB, as well as, widespread fibrin deposition in the contralateral hemisphere that was not subjected to laser illumination (data not shown).

2. The authors need to address whether thrombin injection will affect blood coagulation and cause small thrombi in the brain?

This is another excellent point that is similar to Reviewer 1's Major Concerns. Please see the results for reviewers' perusal in addressing Reviewer 1's comments, and we have included the findings as a Note to step 3.6, as stated above.

In conclusion, we are grateful for the positive and constructive comments by the editors and both reviewers, and have strived to improve our manuscript following these comments. We hope the revised manuscript is deemed satisfactory and suitable for publication in JoVE. Thank you!



blood advances[®]

MENU ▾

Copyright Information

As the open-access journal of the American Society of Hematology, *Blood Advances* makes the full text of every article published in the journal immediately accessible online, www.bloodadvances.org.

All material published in *Blood Advances* represents the opinions of the authors and does not reflect the opinions of the [American Society of Hematology](#), the Editors, or the institutions with which the authors are affiliated. Authors submitting manuscripts to *Blood Advances* do so with the understanding that if a manuscript is accepted, the copyright in the article, including the right to reproduce the article in all forms and media, shall be assigned exclusively to The American Society of Hematology and that the corresponding author and all coauthors will be required to sign their copyright transfer using *Blood Advances* [eJournalPress](#). The American Society of Hematology does not provide a Creative Commons license.

Blood Advances allows authors to retain a number of nonexclusive rights to their published article. The work of the authors who are U.S. Federal Government employees is not protected by the Copyright Act, and copyright ownership will not be transferred in these cases. The online form to sign on *Blood Advances* [eJournalPress](#) allows authors to indicate their status as Federal Government employees.

Authors have permission to share their work in the following ways after their article has been published online in *Blood Advances*.

- With students or colleagues for their personal use in presentations and other educational endeavors.
- On the authors' institutional repositories.
- On personal websites.
- As a link to the article on the journal's website anywhere at any time.
- Publicly on non-commercial platforms.

[Skip to Main Content](#)

Specific examples of acceptable author reuse and sharing include:

- Reprinting the article in print collections of the author's own writing.
- Reusing figures and tables created by the author in future works.
- Reproducing the article for use in courses the author is teaching. If the author is employed by an academic institution, that institution may also reproduce the article for course teaching.
- Distributing photocopies of the article to colleagues, but only for non-commercial purposes.
- Posting a copy of the article on the author's personal website, departmental website, and/or the university intranet. A hyperlink to the article on the *Blood Advances* website must be included.
- Presenting the work orally in its entirety.
- Using the article in theses and/or dissertation.

Authors reusing their own material in the above ways must include appropriate attribution and do not need to contact Blood Advances for permission. For all other uses, the author must request permission from ASH by [visiting the Copyright Clearance Center](#).

© *Blood Advances* Online by the American Society of Hematology

Advertisement

[Skip to Main Content](#)

[Current Issue](#)

[Latest Articles](#)

[Collections](#)

[Community Conversations](#)

[Blood Advance Talks](#)

[All Issues](#)

[Newsroom](#)

[Copyright](#)

[Permissions](#)

[Submit to Blood Advances](#)

[Alerts](#)

[Contact Us](#)

[Order Reprints](#)

[Advertising in Blood Advances](#)

[Authors](#)

[Twitter](#)

American Society of Hematology / 2021 L Street NW, Suite 900 / Washington, DC 20036 /
TEL +1 202-776-0544 / FAX +1 202-776-0545

ASH Publications

Blood

Blood Advances

Hematology, ASH Education Program

ASH Clinical News

ASH-SAP

The Hematologist

[Skip to Main Content](#)

American Society of Hematology

[ASH Home](#)
[Research](#)
[Education](#)
[Advocacy](#)

[Meetings](#)
[Publications](#)
[ASH Store](#)

Copyright ©2020 by American Society of Hematology

[Privacy Policy](#)

[Cookie Policy](#)

[Terms of Use](#)

[Contact Us](#)